Molecular Structures of the η^4-Tetraphenylcyclobutadiene Complexes $MCp(\eta^4\text{-}C_4Ph_4)Cl_2$ (M = Nb, Mo) and Their Relationship to Bent-Sandwich MCp_2Cl_2 Complexes

Owen J. Curnow, Wakgari Hirpo, William M. Butler, and M. David Curtis*

Department of Chemistry, University of Michigan, Ann Arbor, Michigan 48109-1055

Received June 25, 1993®

The structures of the η^4-tetraphenylcyclobutadiene complexes $MCp(\eta^4\text{-}C_4Ph_4)Cl_2$ (M = Nb (**1**), Mo (**2**)), when compared to the bent-sandwich complexes MCp_2Cl_2, are consistent with the LUMO of d^0 complexes and the HOMO of d^1 and d^2 complexes of both types being in the MCl_2 plane and parallel to the Cl–Cl vector. Extended Huckel calculations are consistent with this interpretation and also show that the η^4-cyclobutadiene ligand is best represented as a dinegative ligand when formal oxidation states are assigned. The EHMO calculations were also used to account for the various factors that influence the Cl–M–Cl bond angle. In particular, the Cl–M–Cl angles are found to decrease as the d electron count increases (97.3(1)° for **1** (d^0) and 90.0(1)° for **2** (d^1)). Crystal data for **1**: monoclinic, space group $P2_1/n$; $Z = 4$; $a = 11.138(3)$ Å, $b = 14.584(5)$ Å, $c = 16.305(6)$ Å, $\beta = 94.36(3)°$; $V = 2641(1)$ Å^3; $T = 295$ K; $R = 0.0295$; $R_w = 0.0292$ based on 2763 reflections for $F_o \geq n\sigma(F_o)$ ($n = 3$). Crystal data for **2**: orthorhombic, space group *Pbca*; $Z = 8$; $a = 27.118(39)$ Å, $b = 11.420(12)$ Å, $c = 19.322(15)$ Å; $V = 5984(11)$ Å^3; $T = 295$ K; $R = 0.057$; $R_w = 0.057$ based on 1824 reflections for $F_o \geq n\sigma(F_o)$ ($n = 3$).

Introduction

Compounds of the formula MCp_2L_n ($n = 1$–3) have been extensively studied, both experimentally and theoretically. The earliest MO description was proposed by Ballhausen and Dahl[1] to explain the properties of Cp_2MoH_2. In this model the Mo d^2 electrons were proposed to be in a lone pair directed between the two H atoms. Alcock,[2] in explaining the small Me–Re–Me angle (79°) in $Cp(C_5H_5\text{-}Me)ReMe_2$, proposed that the Re d^2 electrons be in an orbital outside of the $ReMe_2$ triangle (Figure 1). An extensive series of studies by Dahl *et al.* using ESR, X-ray diffraction, PES, and Fenske–Hall calculations on MCp_2L_2 systems, in particular M = Ti and V and $L_2 = Cl_2$, $(SPh)_2$, and S_5, showed experimental evidence consistent with the LUMO of d^0 compounds and HOMO of d^1 and d^2 compounds being composed of primarily $3d_{z^2}$ character with significant contributions from $3d_{x^2-y^2}$ and from the p orbitals on the ligands.[3] EHMO calculations by Hoffmann *et al.* corroborated these conclusions.[4]

In the course of our studies of early transition metal alkyne complexes, we have synthesized the η^4-tetraphenylcyclobutadiene complexes $MCpCl_2(\eta^4\text{-}C_4Ph_4)$, where M = Nb (**1**) or Mo (**2**). In this paper we report their structures and make comparisons with complexes of the formula MCp_2Cl_2. The Mo complex **2** was also reported in an earlier communication.[5]

Experimental Section

General Information. All reactions and manipulations were carried out under a nitrogen atmosphere by use of standard Schlenk line techniques or in an oxygen-free glovebox. All solvents were dried and distilled before use; toluene, di-*n*-butyl ether, and THF were distilled from Na/benzophenone, while CH_2Cl_2 and hexane were distilled from CaH_2. The compounds $MoCpCl(PhCCPh)_2$[6] and $NbCpCl_4$[7] were prepared as previously reported. NMR spectra were recorded on a Bruker AM-300 spectrometer, and ESR spectra were obtained on a Bruker ER-200 spectrometer. Mass spectra were collected on a VG-70-250-S high-resolution mass spectrometer. Elemental analyses were carried out by Galbraith Laboratories Inc., Knoxville, TN.

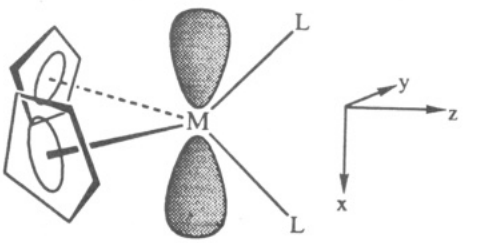

Figure 1. LUMO of d^0, or HOMO of d^1 and d^2, MCp_2L_2 complexes (Allcock–Green model).

$NbCp(\eta^4\text{-}C_4Ph_4)Cl_2$ (1). $NbCpCl_4$ (2.52 g, 8.41 mmol), PhCCPh (1.59 g, 8.93 mmol), Al (0.46 g, 17.0 mmol), and a few milligrams of $HgCl_2$ were loaded into a 500-mL flask, and 250 mL of THF was added. The solution was stirred vigorously for 9 h and then filtered through Celite. After the THF was removed *in vacuo*, the dark red solid was dissolved in toluene and the resulting solution was layered with di-*n*-butyl ether. After 1 week, 0.25 g (0.43 mmol, 10% yield based on PhCCPh) of dark green crystals were obtained. ^1H NMR (C_6D_6): δ 7.40 (dd, *o*-Ph*H*), 7.06 (dd, *m*-Ph*H*), 6.92 (tt, *p*-Ph*H*), 5.75 (s, Cp*H*), $J_{o\text{-}m} = 8.39$ Hz, $J_{o\text{-}p} = 1.26$ Hz, $J_{m\text{-}p} = 7.40$ Hz. ^{13}C NMR (C_6D_6): δ 134.81 (quaternary Ph), 130.15 (*o*-Ph*H*), 128.14 (*m*-Ph*H*), 127.51 (*p*-Ph*H*), 116.42 (Cp*H*), the resonances from the quaternary cyclobutadienyl carbons were not observed. Mass spectrum [*m*/*z* (relative intensity ^{35}Cl)]: 584 (55) M^+, 549 (21) $[M - Cl]^+$, 371 (55) $[CpNbCl(PhCCPh)]^+$, 356 (72) $[C_4Ph_4]^+$, 228 (9) $[M - C_4$-

® Abstract published in *Advance ACS Abstracts,* October 15, 1993.

(1) Balhausen, C. J.; Dahl, J. P. *Acta. Chem. Scand.* **1961**, *15*, 1333.
(2) Alcock, N. W. *J. Chem. Soc. A* **1967**, 2001.
(3) (a) Petersen, J. L.; Dahl, L. F. *J. Am. Chem. Soc.* **1975**, *97*, 6416. (b) Petersen, J. L.; Dahl, L. F. *J. Am. Chem. Soc.* **1975**, *97*, 6422. (c) Petersen, J. L.; Lichtenberger, D. L.; Fenske, R. F.; Dahl, L. F. *J. Am. Chem. Soc.* **1975**, *97*, 6433. (d) Muller, E. G.; Watkins, S. F.; Dahl, L. F. *J. Organomet. Chem.* **1976**, *111*, 73. (e) Muller, E. G.; Petersen, J. L.; Dahl, L. F. *J. Organomet. Chem.* **1976**, *111*, 91.
(4) Lauher, J. W.; Hoffmann, R. *J. Am. Chem. Soc.* **1976**, *98*, 1729.
(5) Hirpo, W.; Curtis, M. D. *J. Am. Chem. Soc.* **1988**, *110*, 5218.
(6) Davidson, J. L.; Green, M.; Stone, F. G. A.; Welch, A. J. *J. Chem. Soc., Dalton Trans.* **1976**, 738.
(7) Bunker, M. J.; De Cian, A.; Green, M. L. H. *J. Chem. Soc., Chem. Commun.* **1980**, 2155.

0276-7333/93/2312-4479$04.00/0

Table I. Crystal, Data Collection, and Refinement Parameters for $NbCp(\eta^4\text{-}C_4Ph_4)Cl_2$ (1) and $MoCp(\eta^4\text{-}C_4Ph_4)Cl_2$ (2·CH_2Cl_2)

	1	2
Crystal Data		
formula	$C_{33}H_{25}Cl_2Nb$	$C_{33}H_{25}Cl_2Mo{\cdot}CH_2Cl_2$
fw	585.4	673.3
cryst dimens, mm	0.33 × 0.34 × 0.38	0.21 × 0.32 × 0.39
cryst syst	monoclinic	orthorhombic
space group	$P2_1/n$ (No. 14)	*Pbca* (No. 61)
Z	4	4
a, Å	11.138(3)	27.118(39)
b, Å	14.584(5)	11.420(12)
c, Å	16.305(6)	19.322(15)
α, deg	90.00(3)	90.00
β, deg	94.36(3)	90.00
γ, deg	90.00(3)	90.00
V, Å^3	2641(1)	5984(11)
D(calc), g/cm^3	1.47	1.495
μ(Mo Kα), cm^{-1}	6.19	8.10
T(max), T(min)	0.81, 0.58	0.84, 0.64
$R(F)$, $R_w(F)$, %	2.95, 2.92	5.7, 5.7
Data Collection		
diffractometer	Syntex $P2_1$	
radiation; λ, Å	Mo Kα; 0.710 73	
monochromator	graphite	
temp, K	295	
2θ(max), deg	45	40
data collcd (h,k,l)	+11,±15,±17	+23,+10,+20
no. of rflns collcd	4095	3425
no. of unique rflns	3471	3425
no. of indpt obsvd rflns $F_o \geq n\sigma(F_o)$	2763 (n = 3)	1824 (n = 3)

$Ph_4]^+$, 193 (14) $[CpNbCl]^+$, 178 (100) $[PhCCPh]^+$. Anal. Calcd for $C_{33}H_{25}Cl_2Nb$: C, 67.7; H, 4.30. Found: C, 67.7; H, 4.26.

$MoCp(\eta^4\text{-}C_4Ph_4)Cl_2$ (2). (a) $MoCpCl(PhCCPh)_2$ (0.70 g, 1.3 mmol) was dissolved in toluene (30 mL), and the solution was heated to reflux for 24 h. After cooling, the solvent was removed *in vacuo* and the green/yellow residue washed with hexane (3 × 10 mL). Brown crystals of the major product $MoCp(\eta^2\text{-}C_4Ph_4)Cl$ were obtained by cooling a concentrated CH_2Cl_2 solution.[5] Chromatography of the supernatent liquid on a silica gel column (2 × 10 cm) with CH_2Cl_2 eluted first a green fraction of $[MoCpCl]_2(\mu\text{-}\eta^4\text{-}C_4Ph_4)$ in 30% yield and then a green fraction that was concentrated to a volume of 5 mL. This solution was layered with 5 mL of toluene to afford 2 in 5% yield after standing at ambient temperature for 24 h. (b) $[MoCpCl]_2(\mu\text{-}\eta^4\text{-}C_4Ph_4)$[5] (0.2 g, 0.27 mmol) in toluene (20 mL) was heated to 95–100 °C for 24 h. The solvent was then removed *in vacuo* and the residue taken up in CH_2Cl_2. After the solution was passed through a silica gel column (4 × 2 cm), compound 2 was obtained in 29% yield by recrystallization from CH_2Cl_2/hexane. ESR (CH_2Cl_2, 20 °C): g = 2.005, A(Mo) = 36 G. Mass spectrum (EI 70 eV): $M^+ = m/z$ 589 with a $MoCl_2$ pattern. Anal. Calcd for $C_{33}H_{25}Cl_2Mo{\cdot}CH_2Cl_2$: C, 60.65; H, 4.04. Found: C, 61.08; H, 4.03.

Collection and Reduction of X-ray Data. Crystal, data collection, and refinement parameters are collected in Table I. The unit cell parameters were obtained from the least squares fit of 15 reflections from the automatic centering routine. An absorption correction was applied to 1 using Gaussian integration, while no corrections were necessary for 2. The structure of 1 was solved from the second EEES map obtained from the SHELX system,[8] while 2 was solved using MITHRIL.[9] In the full-matrix least squares refinement, all non-hydrogen atoms were treated anisotropically and all hydrogen atoms were included in their calculated positions (d(CH) = 1.08 Å, U = 0.05 Å^2). Tables II and III contain the fractional atomic coordinates for 1 and 2, respectively, Table IV contains selected bond distances and angles, and Figures 2 and 3 show the atom labeling schemes for 1 and 2, respectively.[10]

Table II. Fractional Atomic Coordinates (×10^4) and Equivalent Isotropic Thermal Parameters (Å^2 × 10^3) for $NbCp(\eta^4\text{-}C_4Ph_4)Cl_2$ (1)

atom	x	y	z	U
Nb1	−703(1)	4329(1)	2036(1)	32
Cl1	1086(1)	4385(1)	2942(1)	48
Cl2	236(1)	3964(1)	812(1)	56
C1	−1626(3)	3411(2)	2906(2)	31
C2	−2365(3)	3351(3)	2118(2)	33
C3	−1460(3)	2758(2)	1793(2)	31
C4	−743(3)	2798(3)	2562(2)	32
C11	−1933(3)	3530(2)	3769(2)	32
C12	−2923(4)	3064(3)	4040(2)	43
C13	−3214(4)	3135(3)	4851(3)	52
C14	−2532(5)	3670(3)	5397(3)	57
C15	−1548(5)	4120(3)	5146(2)	62
C16	−1247(4)	4052(3)	4334(2)	51
C21	−3666(3)	3471(3)	1924(2)	38
C22	−4262(4)	3047(3)	1240(3)	49
C23	−5515(4)	3137(4)	1093(3)	66
C24	−6173(4)	3633(4)	1613(3)	66
C25	−5593(4)	4050(3)	2297(3)	61
C26	−4355(4)	3980(3)	2444(3)	47
C31	−1398(3)	2180(3)	1060(2)	34
C32	−981(3)	1291(3)	1151(2)	35
C33	−1022(4)	692(3)	487(2)	47
C34	−1470(4)	998(3)	−279(3)	54
C35	−1862(4)	1889(3)	−386(2)	51
C36	−1826(4)	2480(3)	272(2)	44
C41	261(3)	2240(3)	2915(2)	32
C42	164(4)	1808(3)	3672(3)	44
C43	1039(4)	1197(3)	3976(3)	54
C44	2029(4)	1011(3)	3539(3)	54
C45	2150(4)	1451(3)	2801(3)	53
C46	1276(3)	2064(3)	2491(2)	41
C51	−468(4)	5951(3)	1681(4)	62
C52	−753(5)	5925(3)	2493(4)	70
C53	−1903(5)	5534(3)	2521(3)	66
C54	−2335(4)	5349(3)	1700(3)	58
C55	−1448(4)	5611(3)	1196(3)	56

Results and Discussion

The complex $NbCp(\eta^4\text{-}C_4Ph_4)Cl_2$ (1) was obtained unexpectedly from one attempted synthesis of $NbCp(PhCCPh)Cl_2$ by reduction of $NbCpCl_4$ with $Al/HgCl_2$ in the presence of PhCCPh.[11] Attempts to repeat the synthesis have been unsuccessful. The analogous paramagnetic 17-electron complex $MoCp(\eta^4\text{-}C_4Ph_4)Cl_2$ was initially obtained in small yield from the thermal decomposition of $MoCp(PhCCPh)_2Cl$ in toluene. The other products were the expected $MoCp(\eta^2\text{-}C_4Ph_4)Cl$ that contains a bent metallacyclopenta*tri*ene ring and $Mo_2Cp_2Cl_2(\mu_2\text{-}\eta^4\text{-}C_4Ph_4)$ (3), featuring a structure that may be best described as containing a bicapped, tetrahedral Mo_2C_4 core.[5] The thermal decomposition of toluene solutions of 3 followed by crystallization of the reaction mixture from methylene chloride was found to give a higher yield synthesis of 2. The second chlorine atom in 2 arises from a reaction of an as yet unidentified intermediate with CH_2Cl_2. The toluene reaction mixture does not show the characteristic ESR signal of 2 until the CH_2Cl_2 has been added.

The ORTEP[10] diagrams of $NbCp(\eta^4\text{-}C_4Ph_4)Cl_2$ (1) (Figure 2) and $MoCp(\eta^4\text{-}C_4Ph_4)Cl_2$ (2) (Figure 3) display the pseudotetrahedral geometry of these complexes where-

(8) Sheldrick, G. M. *SHELX-76, a Program for Crystal Structure Determination*; University of Cambridge: Cambridge, England, 1976.
(9) Gilmore, C. J. *MITHRIL, contained in TEXSAN, Crystal Structure Analysis Package*; Molecular Structure Corp.: The Woodlands, TX, 1983.
(10) Johnson, C. K. *ORTEP, a thermal ellipsoid drawing program*; Oak Ridge National Laboratories: Oak Ridge, TN, 1971.
(11) Curtis, M. D.; Real, J.; Kwon, D. *Organometallics* **1989**, *8*, 1644.

Table III. Fractional Atomic Coordinates ($\times 10^4$) and Equivalent Isotropic Thermal Parameters ($Å^2 \times 10^3$) for $MoCp(\eta^4\text{-}C_4Ph_4)Cl_2$ ($2\cdot CH_2Cl_2$)

atom	x	y	z	U
Mo1	4212(1)	5236(1)	1760(1)	32
Cl1	4447(1)	4173(3)	2794(2)	43
Cl2	3967(2)	6874(3)	2457(2)	53
C1	3700(5)	3664(13)	1606(7)	32
C2	3429(5)	4588(12)	1953(7)	25
C3	3448(5)	5300(12)	1314(6)	24
C4	3695(5)	4312(12)	971(7)	27
C11	3805(5)	2407(11)	1755(8)	33
C12	4259(6)	1878(13)	1651(7)	45
C13	4226(6)	696(17)	1757(9)	57
C14	3935(9)	5(13)	1942(8)	63
C15	3476(7)	500(15)	2067(8)	57
C16	3416(6)	1692(13)	1953(8)	44
C21	3178(5)	4683(14)	2617(7)	30
C22	3213(5)	3851(13)	3117(7)	37
C23	2969(6)	3939(16)	3740(8)	51
C24	2663(6)	4892(19)	3846(8)	61
C25	2629(6)	5768(15)	3367(9)	57
C26	2878(6)	5665(13)	2723(7)	41
C31	3138(6)	6277(12)	1048(7)	35
C32	2631(6)	6012(13)	904(8)	45
C33	2341(6)	6803(16)	600(9)	48
C34	2527(8)	7886(17)	426(8)	57
C35	3008(7)	8126(13)	563(10)	58
C36	3319(5)	7359(15)	881(8)	48
C41	3764(5)	4079(13)	236(7)	27
C42	3630(5)	4856(14)	-263(8)	42
C43	3683(6)	4640(17)	-973(7)	49
C44	3889(6)	3578(18)	-1163(7)	46
C45	4024(5)	2787(13)	-681(8)	38
C46	3966(6)	2988(13)	23(7)	38
C51	4574(6)	5840(20)	730(8)	53
C52	4794(6)	4795(16)	909(8)	45
C53	5053(6)	4915(17)	1519(8)	54
C54	4985(6)	6121(17)	1729(8)	54
C55	4701(6)	6679(15)	1226(10)	60
C60	4066(9)	6021(18)	4196(9)	117
Cl3	4160(3)	5290(6)	4979(3)	155
Cl4	4321(4)	7354(6)	4233(4)	215

Table IV. Selected Bond Distances and Bond Angles for $NbCp(\eta^4\text{-}C_4Ph_4)Cl_2$ (1) and $MoCp(\eta^4\text{-}C_4Ph_4)Cl_2$ ($2\cdot CH_2Cl_2$)

	1	2		1	2
		Bond Distances (Å)			
M–C11	2.390(1)	2.423(4)	M–C12	2.382(1)	2.398(04)
M–C51	2.455(4)	2.324(15)	M–C1	2.255(4)	2.289(13)
M–C52	2.447(4)	2.335(14)	M–C2	2.349(4)	2.279(13)
M–C53	2.381(4)	2.358(15)	M–C3	2.463(4)	2.246(12)
M–C54	2.381(4)	2.329(14)	M–C4	2.393(4)	2.324(13)
M–C55	2.428(4)	2.354(14)	C51–C52	1.386(7)	1.379(21)
C1–C2	1.476(5)	1.450(18)	C52–C53	1.405(7)	1.397(22)
C2–C3	1.458(5)	1.478(17)	C53–C54	1.413(7)	1.379(19)
C3–C4	1.435(5)	1.471(17)	C54–C55	1.386(6)	1.447(22)
C4–C1	1.471(5)	1.432(17)	C55–C51	1.390(6)	1.395(21)
C1–C11	1.484(5)	1.492(19)	C2–C21	1.469(5)	1.457(17)
C3–C31	1.469(5)	1.488(18)	C4–C41	1.465(5)	1.457(18)
M–Cp[a]	2.11	2.02	M–Cb[b]	2.13	2.04
		Bond Angles (deg)			
C11–M–C12	97.3(1)	90.0(1)	Cp[a]–M–Cb[b]	131.1	131.5
Cp[a]–M–C11	107.5	109.4	Cb[b]–M–C11	104.3	102.2
Cp[a]–M–C12	108.0	109.0	Cb[b]–M–C12	103.7	105.0
M–C1–C11	132.6(3)	127.9(9)	C2–C1–C4	88.7(3)	91(1)
M–C2–C21	133.1(3)	123.7(9)	C1–C2–C3	89.8(3)	90(1)
M–C3–C31	128.9(3)	133(1)	C2–C3–C4	90.7(3)	88(1)
M–C4–C41	128.6(3)	130.2(9)	C1–C4–C3	90.8(3)	91(1)

[a] Cp = centroid of atoms C51 to C55. [b] Cb = centroid of atoms C1 to C4.

in two chloro ligands and the centroids of the two rings each occupy a vertex.

The orientation of the C_4Ph_4 ligand differs somewhat in the two complexes, presumably as a result of crystal packing effects: In **2** the C_4Ph_4 ligand is staggered with respect to the Cl ligands (6° from perfect staggering), while in **1** it is 19° away from being eclipsed. In the crystal, the phenyl rings in **1** adopt a propeller orientation with respect to one another, in which the angles between the normals to the planes of the C_4 ring and the phenyl rings are 53, 8, 44, and 46 for rings 1 through 4, respectively. The phenyl rings in **2**, however, adopt a staggered type of arrangement in which the angles between the normals to the planes of the C_4 ring and the phenyl rings are 59, 4, 70, and 3° for rings 1 through 4, respectively. Possibly as a result of steric interactions with the Cp ligand, the phenyl ring closest to the Cp ligand in each complex (rings 2 and 4 for **1** and **2**, respectively) is twisted the least with respect to the C_4 ring.

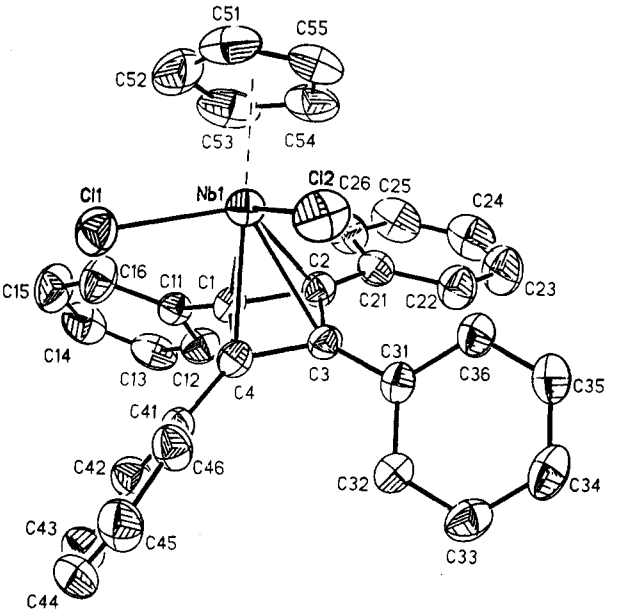

Figure 2. ORTEP plot of $NbCp(C_4Ph_4)Cl_2$ (**1**).

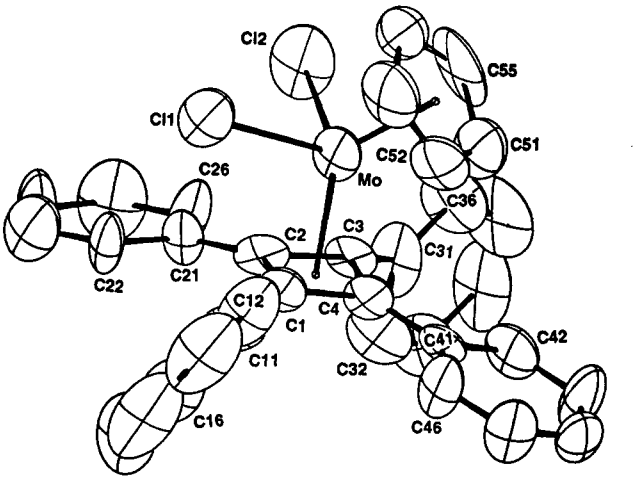

Figure 3. ORTEP plot of $MoCp(C_4Ph_4)Cl_2$ (**2**).

The average Nb–C distance for the Cp ligand of 2.42 Å is not unusual. The average Nb–C distance for the C_4Ph_4 ligand is shorter at 2.37 Å, due to the smaller size of the C_4 ring. These distances are comparable to those observed in the complex $NbCp(C_4Ph_4)(PhCCPh)(CO)$ (2.44 and 2.38 Å, respectively).[12] The corresponding average distances in **2** are approximately 0.1 Å shorter, as is expected from

(12) Nesmeyanov, A. N.; Gusev, A. I.; Pasynskii, A. A.; Anisimov, K. N.; Kolobova, N. E.; Struchkov, Yu. T. *J. Chem. Soc., Chem. Commun.* **1969**, 739.

Table V. Structural Parameters for $MCpC^{\#}Cl_2$[a] Compounds

compd	d^n	M–Cl, Å	Cl–M–Cl, deg	C#–M–Cp, deg	ref
$ZrCp_2Cl_2$	d^0	2.44	97.2	127	15
$NbCp(C_4Ph_4)Cl_2$	d^0	2.39	97.3	131.1	
$NbCp_2Cl_2$	d^1	2.47	85.6	129.3	15
$MoCp(C_4Ph_4)Cl_2$	d^1	2.41	90.0	131.5	
$[MoCp_2Cl_2]^+$	d^1	2.39	87.9	131.5	15
$MoCp_2Cl_2$	d^2	2.47	82.0	130.6	15

[a] C# = C_5H_5 or C_4Ph_4 centroid.

the smaller covalent radius of Mo, and show the same trends (2.34 and 2.28 Å for Mo–C(C_5 ring) and Mo–C(C_4 ring), respectively).

A question arises as to whether the C_4Ph_4 ligand is neutral or dinegative. As a neutral ligand, the Nb atom would be in a +3 oxidation state and have a d^2 electron configuration. As a dinegative ligand, the Nb atom would be in a +5 oxidation state and have a d^0 electron configuration. The ^{13}C NMR spectrum favors a Nb(V) species: the Cp ^{13}C resonance at 116.4 ppm is similar to that of the Nb(V) compound $CpNbCl_2(MeC_6H_4CCC_6H_4Me)$[11] (112.4 ppm). A Nb(IV) compound, $[CpNb(\mu\text{-}Cl)(MeC_6H_4CCC_6H_4Me)]_2$, has the Cp ^{13}C resonance at 102.8 ppm,[13] while the Nb(II) compound $[(C_5H_4Me)Nb(\mu\text{-}Cl)(CO)_2]_2$ has resonances at 95.9 and 88.9 ppm for the secondary Cp carbons.[13] The formal oxidation states in the above mentioned complexes are assigned by assuming the alkyne ligands are dinegative anions in accordance with conclusions based on previous observations and calculations.[11]

Compound **2** is paramagnetic with a formal electron count of 17. Its ^1H-NMR spectrum was not observable at ambient temperature (in agreement with the earlier reported butadiene analogue[14]). An ESR spectrum at ambient temperature showed a g value of 2.005 and a hyperfine splitting, A = 36 G, due to coupling with the spin $^5/_2$ nuclei of the Mo atom ($^{95,97}Mo$).

The similarity of the M–Cl bond distances of 2.39 Å for **1** and 2.41 Å for **2** is consistent with the LUMO of **1** and HOMO of **2** containing some p π antibonding character; as the d electron count increases, the M–Cl bonds should lengthen but this is offset by the decrease in the covalent radius of the metal. Similarly, for the series of MCp_2Cl_2 (M = Zr, Nb, Mo) compounds, the M–Cl distance is approximately constant at about 2.46 Å.

EHMO Calculations and the X–M–X Angle. The major structural effect of the added electron on going from $NbCp(\eta^4\text{-}C_4Ph_4)Cl_2$ to $MoCp(\eta^4\text{-}C_4Ph_4)Cl_2$ is the decrease in the Cl–M–Cl angle from 97.3(1) to 90.0(1)°. These angles are consistent with d^0 and d^1 configurations for the metal atoms in Cp_2MX_2 type structures. For the series of analogous compounds in Table V it can be seen that the Cl–M–Cl angle decreases as the d electron count increases: d^0 (~97°) > d^1 (~88°) > d^2 (~82°). The number of d electrons has little effect on the Cp–M–Cp or Cp–M–(C_4Ph_4) angles (see Table V), and there appears to be no significant steric differences between the Cp liand and the C_4Ph_4 ligand. Thus, in compounds **1** and **2**, the $C_4Ph_4^{2-}$ ligand is behaving analogous to a Cp^- ligand.

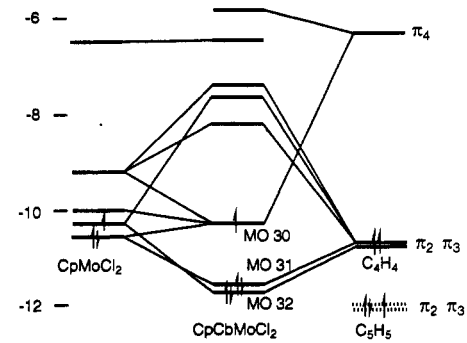

Figure 4. Mo energy level diagram for $CpCbMoCl_2$ as built from $CpMoCl_2$ and Cb (π-C_4H_4) fragments. The location of the π_2,π_3 (e_1) orbitals of Cp is shown for comparison.

The electronic charge distribution of Cp_2MX_2 complexes and the effect of this distribution on the X–M–X angle have been the subject of numerous investigations,[1-4] and this topic continues to attract interest in connection with new structural revelations.[16,17] Green *et al.* made an early extension[18] of the Alcock[2] model, and this experimental picture was buttressed by the early EHMO calculations on Cp_2TiX_2 by Lauher and Hoffmann.[4] These authors computed the energy of Cp_2TiH_2 as a function of the H–Ti–H angle and showed that the population of an orbital of "a_1" symmetry (slightly Ti–H antibonding) caused the H–Ti–H angle to decrease in the order $d^0 > d^1 > d^2$. These authors also explained the preferred orientation of thiolate ligands as a function of the d electron configuration but did not relate the orientations of the thiolate to the S–Ti–S angle.

Calhorda *et al.*[16] have reported EHMO calculations of $Cp_2M(SR)_2$ (M = Ti, Mo) compounds and support their conclusion with thermochemical and structural data. These authors conclude that relief of metal–sulfur π antibonding interactions is the controlling factor in determining the S–M–S angle. Recently, we have shown that a variety of interactions, viz. M–S, S–S, M–Cp, and S-Cp, all are important in setting the S–Ta–S angles in $CpTa(SR)_4$.[19] We were interested in determining to what extent these interactions are involved in setting the X–M–X angle in Cp_2MX_2 or $CpCbMX_2$ complexes. We also wished to determine the effect on the electronic structure of substituting a cyclobutadiene (Cb) ligand for a cyclopentadienyl.

Cb *vs* Cp. Figure 4 shows the interaction of the π-orbitals of the C_4H_4 (Cb) group with the frontier orbitals of the $CpCl_2Mo$ fragment. The orbitals, π_2 and π_3, are the nonbonding, e set of cyclobutadiene. These orbitals form strong covalent interactions with the Mo frontier orbitals and are thus depressed in energy. In neutral $CpCbMoCl_2$, these are filled, and one electron occupies MO no. 30 (see below) which is primarily a metal $d_{z^2-x^2}$ hybrid composed of nearly equal parts of d_{z^2}- and $d_{x^2-y^2}$-orbitals. Thus, the configuration of the metal complex is d^1, i.e. Mo(V), and the Cb group is therefore formally a dinegative ligand. This conclusion is also supported by an analysis of the

(13) Kwon, D.; Real, J.; Curtis, M. D.; Rheingold, A.; Haggerty, B. S. *Organometallics* **1991**, *10*, 143.
(14) Davidson, J. L.; Green, M.; Stone, F. G. A.; Welch, A. J. *J. Chem. Soc., Chem. Commun.* **1977**, 287.
(15) Prout, K.; Cameron, T. S.; Forder, R. A. *Acta. Crystallogr., Sect. B* **1974**, *30*, 2290.
(16) Calhorda, M. J.; de C. T. Carrondo, M. A. A. F.; Dias, A. R.; Frazao, C. F.; Hursthouse, M. B.; Martinho Simoes, J. A.; Teixeira, C. *Inorg. Chem.* **1988**, *27*, 2513.
(17) Darensbourg, M. Y.; Bischoff, C. J.; Houliston, S. A.; Pala, M.; Reibenspies, J. *J. Am. Chem. Soc.* **1990**, *112*, 6905.
(18) Green, J. C.; Green, M. L. H.; Prout, C. K. *J. Chem. Soc., Chem. Commun.* **1972**, 421.
(19) Curnow, O. J.; Curtis, M. D.; Rheingold, A.; Haggerty, B. S. *Inorg. Chem.* **1991**, *30*, 4043.

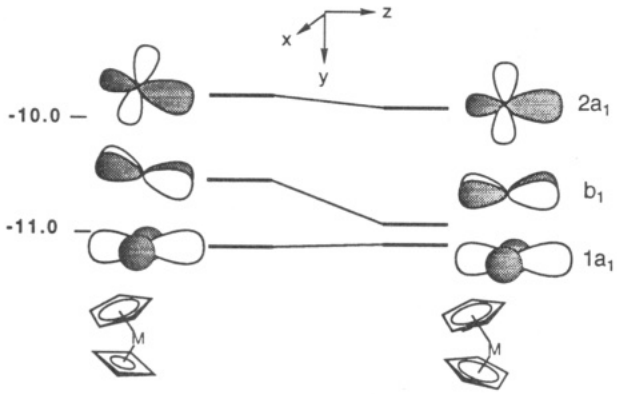

Figure 5. Energies and forms of the frontier orbitals of the CpCbMo and Cp_2Mo fragments.

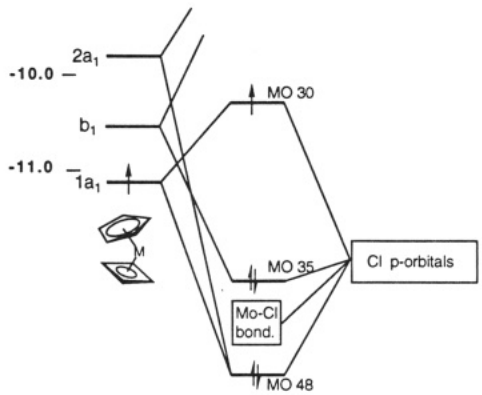

Figure 6. Interaction of CpCbMo frontier orbitals with Cl π-orbitals in $CpCbMoCl_2$.

charge flow: π_2 and π_3 accept 0.45 electron from the $CpCl_2$-Mo fragment. For comparison, the π_2- and π_3-orbitals of Cp, superimposed on Figure 4 for comparison, accept only ca. 0.1 electron. This lower value reflects the fact that in Cp π_2 and π_3 already have one more electron, and also the metal–ligand bonding is not as strong as it is with the Cb ligand (better overlap with the smaller ring). Note that with the one electron more provided by Cp, MO 30 would be doubly occupied, d^2, i.e. Mo(IV).

Another way of comparing Cp and Cb that is germane to the following discussion is illustrated in Figure 5 which shows the frontier orbitals of the CpCbMo and Cp_2Mo fragments. These are the familiar $1a_1$-, b_1-, and $2a_1$-orbitals that have been described previously.[4,18] Other than a slight tilting of the b_1- and $2a_1$-orbitals as a result of the lowered symmetry in CpCbMo and a small shift in energies, the frontier orbitals of Cp_2Mo and CpCbMo are nearly identical. Therefore, the bonding of these two fragments to ligands in the xz-plane will, for all practical purposes, be identical.

$CpCbMoCl_2$. A portion of the MO energy level diagram for $CpCbMoCl_2$ as built from the CpCbMo and Cl_2 fragments is shown in Figure 6. The chlorine p-orbitals lie below the metal d-orbitals, so the Mo–Cl bonding orbitals will have primarily chlorine p character. Two of these Mo–Cl bonding orbitals, labeled MO 35 and MO 48, are diagrammed to the right in Figure 7. MO 30 is formally a Mo–Cl π^*-orbital and is the LUMO for the d^1 configuration. This orbital is also diagrammed in Figure 7.

The Cl–M–Cl Angle. Figure 7 shows the energy variation of MO's 30, 35, and 48 as a function of the Cl–M–Cl angle in $CpCbMoCl_2$. The energy minimum for a d^0 configuration (MO 30 empty) is found at 93°. The

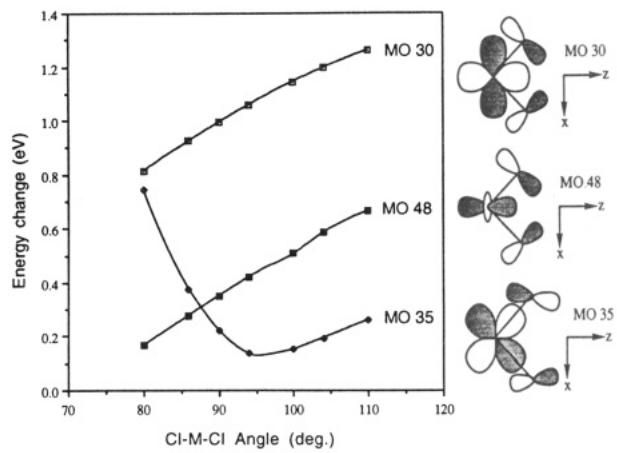

Figure 7. Energies of selected molecular orbitals in $CpCbMoCl_2$ as a function of the Cl–Mo–Cl angle.

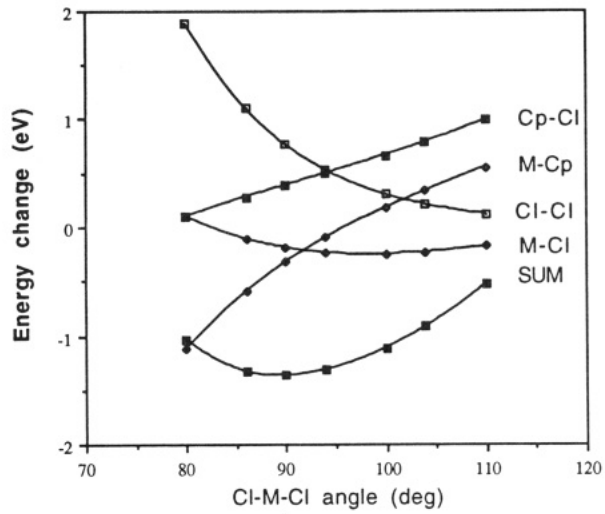

Figure 8. EHMO group interaction energies in $CpCbMoCl_2$ as a function of the Cl–Mo–Cl angle.

population of MO 30 favors a smaller angle: 90° for d^1 and 86° for d^2. The angles in the analogous Cp_2MCl_2 complexes are 91, 88, and 86° for d^0, d^1, and d^2, respectively.

The reason for diagramming MO 35 and MO 48 is that these two molecular orbitals show the largest energy variation as a function of the Cl–M–Cl angle. As this angle decreases from 110°, the energy of Mo 35 falls slightly but then rises steeply as a result of Cl···Cl antibonding interactions. MO 48, on the other hand, drops in energy because a smaller angle enhances M–Cl *and* Cl–Cl bonding in this MO. Since both MO 35 and MO 48 are occupied, the energy is minimized near 93°. The energy of MO 30 drops as the Cl–M–Cl angle decreases because M–Cl antibonding is relieved and the Cl–Cl *bonding* interaction increases at a low angle.

The foregoing analysis emphasizes M–X and X–X interactions and essentially parallels arguments that were made previously for Cp_2MX_2 complexes.[4,16] However, other interactions are also important. Figure 8 shows the energy variations of group interactions as a function of the Cl–M–Cl angle. The metal–chlorine energy is relatively flat and is not particularly important in determining the MCl_2 angle. The Cp–Cl interaction favors a small Cl–M–Cl angle because the chlorine atoms move toward the more open face of the Cp_2Mo fragment at low angle where filled shell–filled shell ("steric") repulsions are minimized. The Cl–Cl interaction increases significantly at a small

angle, again due to steric repulsions. The surprising aspect of the data in Figure 8 is the decrease in the M–Cp energies at a low MCl_2 angle; i.e. the Mo–Cp bonding is better when the Cl–M–Cl angle is compressed. We believe this effect is due to a rehybridization of the d-orbitals that occurs as the chlorine atoms are moved closer together. At low angles, some of the d-orbitals are "pushed back" and overlap better with the Cp carbon atoms on the back side or closed face of the sandwich complex. The sum of all these interactions, shown in Figure 8, has a minimum at 90° for a d^1 configuration.

Although we have not made any calculations of thiolate complexes, $Cp_2M(SR)_2$, the reason behind the large differences in the S–M–S angle as a function of the exo–endo conformation of the –SR ligands is clear. The S–M–S angle in exo complexes ranges from 71 (d^2) to 79° (d^1), whereas the endo conformations show larger values, ca. 100 (Nb^+, d^0) to 89° (V, d^1).[16,17] The exo conformation places the sulfur lone pairs more or less parallel to the x-axis and to one another. The endo conformation orients the sulfur lone pairs toward one another, and this leads to more lone pair–lone pair repulsion and to larger S–M–S angles.

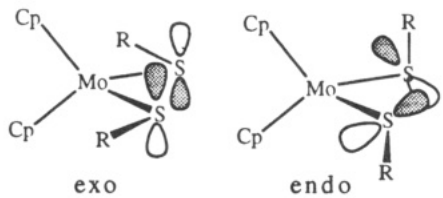

Acknowledgment. We wish to thank the donors of the Petroleum Research Fund, administered by the American Chemical Society, and the National Science Foundation (CHE-8619864) for support of this research.

Appendix

EHMO calculations were performed on the model complexes, $(\eta^5\text{-}C_5H_5)(\eta^4\text{-}C_4H_4)MoCl_2$ and $(\eta^5\text{-}C_5H_5)_2MoCl_2$, using the weighted H_{ij} formula with the program ICON8 by Hoffmann et al.[20] The geometry corresponded to the experimental geometries averaged to C_s or C_{2v} symmetry. The local coordinate system is shown in Figure 1 (z-axis bisecting the Cl–M–Cl angle, y-axis in the ring centroid–M–ring centroid plane, and origin on the metal). The Mo–C(Cp) and Mo–C(Cb) distances were 2.34 and 2.25 Å, respectively, and the Mo–Cl distance was fixed at 2.41 Å. The default parameters for C and H were used, and the parameters for Mo and Cl were as follows: [H_{ii} (eV) for Mo] 5s –8.77, 5p –5.6, 4d –11.06; [H_{ii} (eV) for Cl] 3s –26.3, 3p –14.2; [exponents (ζ) for Mo] 5s 1.96, 5p 1.90, 4d 4.54 (0.58988) and 1.90 (0.58988); [exponents (ζ) for Cl] 3s 2.18, 3p 1.73.

Supplementary Material Available: Tables of anisotropic thermal parameters, H-atom positions, and bond distances and angles for compounds **1** and **2** (9 pages). Ordering information is given on any current masthead page.

OM930430G

(20) Ammeter, J. H.; Burgi, H.-B.; Thibault, J. C.; Hoffmann, R. *J. Am. Chem. Soc.* **1978**, *100*, 3686.